Trajectory-Wise Analysis of Cylindrical and Plane Plasmas in a Magnetic Field and Without Collisions*

LEWI TONKS†

Radiation Laboratory, University of California, Livermore, California

(Received September 19, 1958)

The anatomy of the transition region between vacuum and a fully developed magnetically immobilized ionized-gas plasma has been examined by following particle trajectories in detail. The mathematical formulation has required machine computation for its full interpretation. This approach recognizes the structure imparted to the plasma by the radius of gyration and thus serves as a critique of the magneto-hydrodynamic method. It furnishes the microscopic verification of that macroscopic approach and supplements it by showing that the sharpness of transitions in a plasma are limited, in effect, by the gyration radius in the stronger, not the weaker, magnetic field. Especially, it brings out the greater importance of the tensor character of the plasma pressure in the cylindrical case where the combined kinetic and magnetic energy density in uniform interior regions of the plasma is not equal to the magnetic energy density in the vacuum. The analysis also exhibits the intense mass motion at the surface of a strong plasma constituting a paramagnetic electric current and probably having dynamical effects. The numerical work has been correlated where possible with direct theoretical results.

I. INTRODUCTION

THE earlier work in the Sherwood Project on the magnetohydrodynamics of an ionized plasma used as a favorite device the concept that a magnetically immobilized plasma, when bounded, had a sharp boundary outside of which there lay only vacuum and magnetic field. Certainly diffusion would obliterate the step function in density, and the original attainment of such a step function is probably impossible, but aside from these considerations the question arises as to how thin a transition between vacuum and full plasma density can be in view of the considerable size of an element of plasma structure, namely the diameter of the charged-particle orbit. The analysis which follows was undertaken to throw light on this problem. It keeps the particles in view to a later stage in the analysis. Since this work was done more insight has been gained than then existed into the limitations of the hydrodynamic approach and a new method has been proposed based on distribution functions of the plasma particles which are solutions of the Boltzmann equation without its collision terms. This is, however, only a partial answer because it only transfers the seat of difficulty to the problem of expressing physically plausible distributions in the terms acceptable to the method.

The approach here is more primitive. It is based on the realization that if one imagines proceeding from left to right from a known vacuum magnetic field into an immobilized plasma, one is always in a magnetic field which can be calculated on the basis of trajectories and parts of trajectories already encountered. For this

reason the trajectories can be calculated to be consistent with the field at each point. Position will be described by a single coordinate, radial distance, only. Every trajectory has an apogee, the turning point at which, as one approaches the axis, it is first encountered, and a perigee, the turning point at which it is left behind. Thus at a point in general there will be a multitude of trajectories to be kept track of, namely all those whose apogees but not perigees have been encountered. Although the calculation indicated is sound in principle it becomes unwieldy in practice. The simplification adopted was to confine attention to particles of a single charge e, single mass m, and single speed v perpendicular to the uniform vacuum magnetic field B_0. The first analysis was done for the case where the field lay in the z direction, the plasma face in the y, z plane and the only variations lay in the x direction. The numerical calculations were made for this case. Here it appears reasonable to analyze the cylindrical case with results which reduce easily to the Cartesian case.

II. FORMULATION OF BASIC RELATIONS

Referring to Fig. 1, the vacuum magnetic field B_0 is uniform in the z direction (perpendicular to the paper). The plasma density is assumed to be uniform in the z direction and the plasma lies within a radius r_0. We now define a Class ρ particle. It is one which crosses the element of area $dz d\rho$ (lying at $r=\rho$, $\theta=0$) in the negative θ direction (i.e., clockwise) whose velocity vector lies within a small angle α normal to $\theta=0$, and which traverses $\theta=0$ within a short time interval dt at $t=0$. In the figure, $d\rho$ lies at the apogee, P, and for ease of analysis α extends to the right from the normal to OP. Trajectories 1 and 2 bound the stream of class ρ particles. To within second-order quantities they are congruent to each other, and trajectory 2 may be alternatively looked upon as being trajectory 1 rotated through the angle α about P as center, or as being

trajectory 1 rotated through the angle β about O as center, again to second-order quantities. Since these trajectories are circles in the neighborhood of P,

$$a\alpha = (\rho - a)\beta, \qquad (1)$$

where a is the local radius of gyration (see Fig. 1).

Let the number of class ρ particles be

$$\sigma(\rho)\alpha dt d\rho dz, \qquad (2)$$

the dependence of σ upon ρ being the factor which determines the plasma density as a function of r.

At some instant t the Class ρ particles will occupy the volume $(ABCD)dz$, where

$$AB = vdt.$$

This volume is the same as $(ABC'D')dz$, where BC' and AD' are arcs with the plasma axis O as center, and, as remarked

$$\sphericalangle AOD' = \beta,$$

and

$$AD' = \beta r.$$

This is the base of a parallelogram of which the corresponding height is the radial component of vdt or

$$\dot{r}dt$$

to give a volume

$$\beta r |\dot{r}| dtdz.$$

Putting $n_\rho(r)$ for the particle density of Class ρ particles and equating total number of particles, we get directly

$$n_\rho(r)\beta r |\dot{r}| dtdz = 2\sigma a dt d\rho dz,$$

where the factor 2 recognizes that both outgoing and incoming trajectory branches contribute to density. Then, using Eq. (1), we have

$$n_\rho(r) = 2\sigma(\rho)\left[\frac{\rho - a(\rho)}{a(\rho)}\right]\frac{1}{r\dot{r}}d\rho. \qquad (3)$$

Here it is to be clear that a is the local trajectory radius at ρ only, but that $\dot{r}$ will be a function of ρ as well as r. Of course, σ is a function of ρ only. The absolute-value designation has been taken from $\dot{r}$ with the understanding that the evaluation of n, and later of the current, j_θ, shall be based on the portion of trajectory occurring prior to the apogee, i.e., at negative times, when $\dot{r}$ is intrinsically positive.

As previously, we then have for the total density of all contributing classes

$$n(r) = \frac{2}{r}\int_r^{\rho(r)}\frac{\sigma(\rho)(\rho - a)}{a\dot{r}}d\rho, \qquad (4)$$

and the current density from all contributing classes is

$$j_\theta = 2e\int_r^{\rho(r)}\frac{(\rho - a)\sigma(\rho)}{a}\frac{\dot{\theta}}{\dot{r}}d\rho, \qquad (5)$$
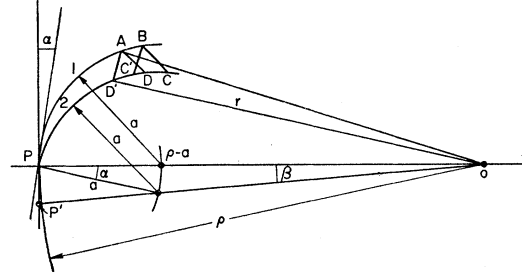
FIG. 1. Trajectory analysis for cylindrical plasma.

where $\rho(r)$ is the apogee of the oldest trajectory passing through r.

III. PRESSURE AS A TENSOR

From Eq. (4),

$$\frac{d}{dr}(n(r)\langle\dot{r}^2\rangle_{Av}) = \frac{2d}{dr}\int_r^{\rho(r)}\frac{(\rho - a)\sigma}{a}\frac{\dot{r}}{r}d\rho.$$

Now the integrand vanishes at the lower limit either because $\dot{r} = 0$ at an apogee or because $\sigma = 0$, and it vanishes at the upper limit because $\dot{r} = 0$ there; accordingly,

$$\frac{d}{dr}(n(r)\langle\dot{r}^2\rangle_{Av}) = 2\int_r^{\rho(r)}\frac{(\rho - a)\sigma}{a}\left(\frac{1}{r}\frac{\partial\dot{r}}{\partial r} - \frac{\dot{r}}{r^2}\right)d\rho.$$

Since

$$\dot{r} = \dot{r}[\rho, r(\rho, t)],$$
$$\ddot{r} = \dot{r}\partial\dot{r}/\partial r, \qquad (6)$$

and using also the trajectory equation:

$$\ddot{r} - r\dot{\theta}^2 = \omega(r)r\dot{\theta} \qquad (7)$$

(where $\omega = eB/mc$, as usual), we obtain

$$\frac{d}{dr}(n(r)\langle\dot{r}^2\rangle_{Av}) = 2\int_r^{\rho(r)}\frac{(\rho - a)\sigma}{a}\left(\frac{\omega\dot{\theta}}{\dot{r}} + \frac{\dot{\theta}^2}{\dot{r}} - \frac{\dot{r}}{r^2}\right)d\rho.$$

Now from Eq. (5), we have

$$\frac{B}{4\pi m}\frac{dB}{dr} = -\frac{\omega(r)j_\theta}{e} = -2\int_r^{\rho(r)}\frac{(\rho - a)\sigma}{a}\frac{\omega\dot{\theta}}{\dot{r}}d\rho.$$

Addition then gives

$$\frac{d}{dr}\left(\frac{B^2}{8\pi} + mn(r)\langle\dot{r}^2\rangle_{Av}\right) = m\int_r^{\rho(r)}\frac{(\rho - a)\sigma}{ar\dot{r}}\frac{(r\dot{\theta})^2 - \dot{r}^2}{r}d\rho, \qquad (8)$$

a relation which will be seen to emphasize the special importance of the tensor character of the pressure in cylindrical geometry.

Equation (8) reduces to the Cartesian case if we let r become infinite keeping $r\dot{\theta}$ finite. The right member

vanishes and we have, directly,

$$(B^2/8\pi)+mn\langle\dot{r}^2\rangle_{\text{Av}}=\text{constant}.$$

This is easily generalized to a range of particle masses and speeds, and it is readily seen that between two regions in each of which B is constant and the plasma motions are isotropic, this becomes rigorously

$$\frac{B_2{}^2-B_1{}^2}{8\pi}+p_2-p_1=0, \tag{9}$$

where p designates the scalar pressure.

Nothing like this is possible with the original Eq. (8), so that transition regions leave their imprint on isotropic regions. The right member of Eq. (8) is directly expressible in terms of tensor components. The first and third factors in the integrand constitute a density increment as can be seen by reference to Eq. (4). Factoring in the second factor thus yields an increment to $(p_{\theta\theta}-p_{rr})/r$, so that Eq. (8) can be alternatively written

$$\frac{d}{dr}\left(\frac{B^2}{8\pi}+p_{rr}\right)+\frac{p_{rr}-p_{\theta\theta}}{r}=0, \tag{10}$$

an equation which can be derived in other ways.

IV. EQUATIONS FOR THE PLANE PLASMA

The conversion of Eqs. (4) and (5) to the plane case is accomplished directly by the substitutions

$$r=X_\infty-x, \quad \eta=X_\infty-\rho,$$

where X_∞ is allowed to approach infinity and η takes the place of ρ in labeling the particular trajectory under observation; we then have

$$n(x)=\frac{2}{v}\int_{\eta(x)}^{x}\frac{\sigma(\eta)\omega(\eta)}{|\dot{x}|}d\eta, \tag{11}$$

$$j_y(x)=-2e\int_{\eta(x)}^{x}\frac{\sigma\omega\dot{y}(\eta,x)}{|\dot{x}|}d\eta \tag{12}$$

for the particle density and current density, respectively, with the coordinate x increasing from left to right. Here also

$$\omega(\eta)=eB(\eta)/(mc). \tag{13}$$

Now by using

$$dB_z/dx=-4\pi j_y/c, \tag{14}$$

and letting the plasma boundary lie at $x=0$, we find the equation for the magnetic field to be

$$B(x)=B_0-\frac{8\pi e}{cv}\int_0^x dx'\int_{\eta(x')}^{x'}\frac{\sigma(\eta)\omega(\eta)\dot{y}(\eta,x')}{|\dot{x}(\eta,x')|}d\eta. \tag{15}$$

The equations of the particle trajectories are the usual

$$\ddot{y}=-\omega\dot{x}; \quad \ddot{x}=\omega\dot{y}. \tag{16}$$

V. EQUATIONS IN DIMENSIONLESS FORM

To put these equations in dimensionless form we make the following substitutions of dimensionless capitals for the lower case variables:

$$\omega=\Omega eB_0/(mc)=\Omega\omega_0, \tag{17}$$

$$t=T/\omega_0, \quad (x,x',\eta,y)=(X,X',H,Y)v_0/\omega_0. \tag{18},(19)$$

The new equations are

$$\Omega(X)=1-\frac{8\pi e^2v}{mc^2\omega_0{}^2}\int_0^X dX'\int_{H(X')}^{X'}\frac{\sigma(vH/\omega_0)\Omega(H)Y}{\dot{X}}dH,\tag{20}$$

$$\frac{d^2Y}{dt^2}+\Omega(X)\frac{dX}{dt}=0, \quad \frac{d^2X}{dt^2}-\Omega(X)\frac{dY}{dt}=0,$$

where

$$\dot{X}\equiv dX/dT, \quad \text{etc.}$$

It only remains to put

$$S(H)=\frac{8\pi e^2v}{mc^2\omega_0{}^2}\sigma(vH/\omega_0)=\frac{8\pi mv}{B_0{}^2}\sigma \tag{21}$$

to make the field equation dimensionless also:

$$\Omega(X)=1-\int_0^X dX'\int_{H(X')}^{X'}\frac{S(H)\Omega(H)\dot{Y}}{\dot{X}}dH. \tag{22}$$

If now we apply the same conversion to Eq. (11) we find

$$n(x)=\frac{B_0{}^2}{4\pi mv^2}\int_{H(X)}^{X}\frac{S(H)\Omega(H)}{|\dot{X}|}dH. \tag{23}$$

In the absence of collisions there is no natural distribution of particles to govern the choice of the build-up function $S(H)$. For orientation purposes $S(H)=S_0$ is probably the most useful choice because it leads into an asymptotically uniform plasma.
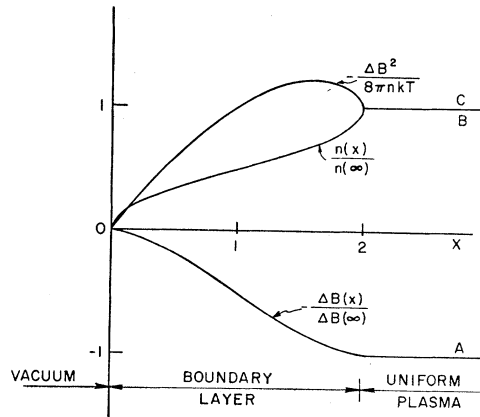
Fig. 2. Density and field distribution in weak Cartesian plasma. $x\equiv X/\omega_0$.

VI. SOLUTION FOR WEAK PLASMAS

The solution of the equations is a machine job and has been done on the Univac. It is worthwhile, however, to solve analytically that order of approximation in which the particle density is so low that the depression of B is so small that the deviation of the trajectories from circular is negligible. Then the orbit radius is unity, and for the trajectory

$$X = H + 1 - \cos T,$$
$$\dot{X} = \sin T, \qquad (24)$$
$$d^2X/dt^2 = \cos T = \dot{Y},$$

and for fixed X

$$dH = -\sin T\, dT.$$

The first integration in Eq. (22) for $S(H) = S$, constant, is conveniently carried out in the two regions

(A) $0 \leq X' \leq 2$:

$$S\int_0^{X'} \frac{(X'-H-1)}{\dot{X}} dH = -S[1-(1-X')^2]^{\frac{1}{2}};$$

(B) $2 \leq X'$:

$$S\int_{X'-2}^{X'} \frac{(X'-H-1)}{\dot{X}} dH = 0.$$

Using

$$\psi = \cos^{-1}(1-X), \quad 0 \leq \psi \leq \pi \qquad (25)$$

the second integration leads to

$$\Omega(X) - 1 = \begin{cases} -\frac{1}{2}S(\psi - \frac{1}{2}\sin 2\psi), & 0 \leq X \leq 2 \\ -\frac{1}{2}S\pi, & 2 \leq X \end{cases} \qquad (26)$$

which represents the depression of the magnetic field in dimensionless form. The quantity $(2/\pi)(\Omega-1)/S = (2/\pi)(\Delta B/B_0 S)$ is plotted against X as Curve A of Fig. 2.

Turning to the particle concentration given by Eq. (23):

$$n(x) = \frac{B_0^2 S}{4\pi m v^2} \times \begin{cases} \psi, & 0 \leq X \leq 2 \\ \pi, & 2 \leq X. \end{cases} \qquad (27)$$

In Fig. 2, $n(x)$ is shown as Curve B, but plotted against X.

Now we can compare the depression in the field to the particle concentration and it will suffice to do this for $0 \leq X \leq 2$ because for $X > 2$ relations remain constant.

$$\frac{\Omega(X)-1}{n(x)} = \frac{dB}{B_0 n} = \frac{2\pi m v^2}{B_0^2}\left(1 - \frac{\sin 2\psi}{2\psi}\right). \qquad (28)$$

The best rough approximation for the introduction of temperatures T is to put

$$mv^2/2 \simeq kT, \qquad (29)$$

whence

$$d(B^2) - 8\pi n k T[1 - \sin 2\psi/(2\psi)] = 0. \qquad (30)$$

For $X > 2$ the bracketed expression should be replaced by its $X = 2$ value, namely, unity, and thus the generally accepted relation is confirmed. Here we have an example of the effect of anisotropy of the plasma causing a departure from the simple condition expressed by Eq. (9). This departure is shown by Curve C of Fig. 2, which is a plot of the negative of the bracket in Eq. (30).

VII. PRESSURE INTEGRAL OF EQ. (22) WITH A SPEED DISTRIBUTION AND ANY PLASMA STRENGTH

Equation (22) can be generalized by including in it a continuum of source terms $S(H,v)dv$ for a range of velocity classes. It is not difficult in this way to arrive rigorously at the result

$$\frac{d}{dx}(B^2 + 8\pi m n \langle \dot{x}^2 \rangle_{\text{Av}}) = 0. \qquad (31)$$

For the Maxwellian case it becomes, as expected,

$$\frac{d}{dx}(B^2 + 8\pi n k T) = 0. \qquad (32)$$

VIII. ELECTRIC CURRENTS AND MASS MOTIONS IN THE BOUNDARY LAYER

At a distance x_p from the plasma edge where the plasma is essentially Maxwellian and uniform (except for the dearth of those high-speed particles which would penetrate the plasma edge) imagine a plane P as shown in Fig. 3. To the right of P trajectories are circular so that there is no mass drift. At any point in that region all directions of motion are equally likely for all velocity classes so that there is no net current density.

We shall be interested in the total current per unit z depth of plasma, and we have just seen that all of it lies to the left of P. There we analyze the electric current not by volume element but by particles in their trajectories. Some trajectories cross P, many do not.
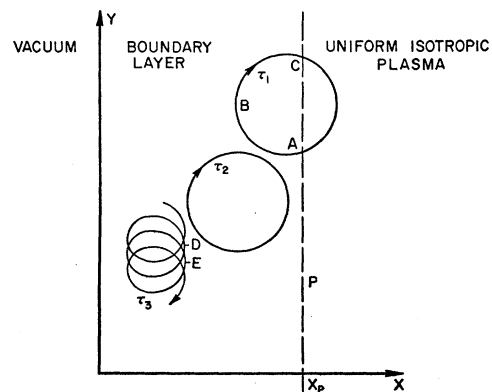
FIG. 3. Analysis of boundary layer currents.

The current, in terms of field depression $\Delta\Omega$, arising. from the former will be denoted by J_1, from the latter by J_2, and precise meaning is given these quantities by writing

$$\Omega-1=J_1+J_2. \tag{33}$$

The cut trajectories are responsible for a current because, as with trajectory τ_1 of Fig. 3 the particle makes its contribution to J_1 by its transport from A via B to C; its transport from C to A is balanced, as we have seen, among all the other particles to the right of P. Particles in circular orbits like τ_2 which lie entirely within the region contribute nothing to J_2, but for particles in trajectories like τ_3 their progress from D to E in each cycle does contribute to J_2.

Now J_1 and J_2 can be separated out of the double integral in Eq. (22). The area of integration is shown as $OABCDEO$ in Fig. 4. Since X_p lies in a uniform region the orbit there is circular, constant in size, and actually of radius (dimensionless) $1/\Omega(X)$; and $H=H(X)$ is parallel to $H=X$. A little reflection will show that reversing the order of integration is physically equivalent (1) to selecting one trajectory ($H=$ constant) and summing its current contributions, and then (2) summing over all the trajectories involved. It then becomes evident that the cut trajectories are those included in the area $CDEC$. For this, the double integral for a single velocity class is

$$J_{1v}=-\int_{Hc}^{Xc+2/\Omega} dX \int_{Hc}^{X} \frac{S(H,v)dv\Omega(H)\dot{Y}dH}{\dot{X}}$$

$$=-\pi S_v/(2\Omega), \tag{34}$$

since $S(H,v)\Omega(H)$ is constant in a uniform plasma‡ and the equations of motion are

$$X=H+\Omega^{-1}(1-\cos\Omega T),\quad \dot{Y}=\Omega^{-1}d^2X/dt^2.$$

We must now determine S_v to be consistent with a Maxwell distribution. Applied to particles of speed v,
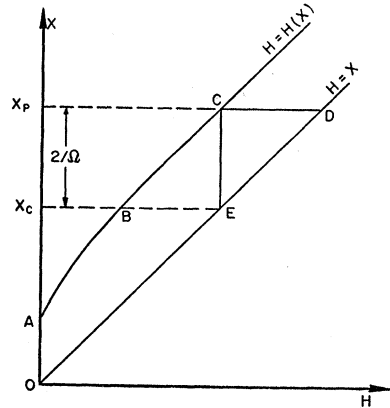
FIG. 4. Integration region.

‡ J_{1v} and S_v are the contributions to J_1 and S, respectively, by particles lying the range dv.

Eq. (23) becomes

$$n_v=\frac{B_0^2 S_v}{4\pi m v^2}2nhm=\exp(-hmv^2)dv,\quad h=1/(2kT).$$

Therefore

$$S=\int_0^{\infty} S_v dv=8nkT/(B_0^2)=(B_0^2-B^2)/(\pi B_0^2).$$

After summing Eq. (34) over all v, we then have

$$J_1=-(1-\Omega^2)/2\Omega, \tag{35}$$

and from Eq. (33)

$$J_2=(1-\Omega)^2/2\Omega. \tag{36}$$

These equations lead to the following comments:

(1) J_2 is a paramagnetic current which is more than overbalanced by the diamagnetic J_1.

(2) In weak enough plasmas where Ω is only slightly less than unity (very slight depression of B) J_2 is negligible compared to J_1 which is a confirmation of the earlier treatment of the weak plasma case.

TABLE I. Weak plasma relations.

S	$\Delta\Omega_\infty=-\frac{1}{2}\pi S$ Theor.	Calc	$\tau=2\pi$ Theor.	Calc	$Y_0=(8/3)S$ Theor.	Calc
0.01	−0.01571	−0.1583	6.28	6.28		
0.03	−0.0471	−0.0485			0.08	0.128

(3) As B is severely depressed, Ω approaching zero, both currents grow without limit.

(4) The current J_2 is associated with a mass motion of the charged particles which will transmit disturbances in one region of the boundary layer to adjacent regions.

(5) These currents must be regarded only with respect to the plasma region to the left of P as a whole. They can be quite misleading as regards the field distribution *within* the boundary layer.

IX. NUMERICAL SOLUTION FOR STRONG PLANE PLASMAS

A. Introduction

In making the numerical solutions the plasma edge lay at $X=0$. To the left, $\Omega=1$, $S=0$, and to the right S was chosen to be a constant because this allowed the plasma to build up to uniformity independent of special behavior of S.

The double space-integral of Eq. (22) makes it necessary that the uniform differences of the integrations shall be space-like and that the time intervals required by the equations of motion be derived from the fundamental space interval ΔX. The machine will calculate the trajectories of those particles which are first encountered at $X=0$, $X=\Delta X$, etc., that is, of

those particles for which $H=n\Delta X$, n integral. Such trajectories will be called reference trajectories.

Near $X=0$ all trajectories are arcs of circles of radius unity, so that in a weak plasma there would be $2/\Delta X$ space intervals in a diameter. Therefore, this is the minimum number of reference trajectories which were "active" at any time once we have penetrated beyond $X=2$. We chose $\Delta X=0.1$. The number of "active" reference trajectories in a field Ω were, therefore, $20/\Omega$.

The integrations were carried out simply on a trapezoidal-rule basis. As a consequence the particle energy showed appreciable build-up with trajectory life, and this was reduced to a fourth-order effect by using

$$\dot{X}_{n+1}=\dot{X}_n[1-\tfrac{1}{2}(\Omega\Delta T)^2]+\Omega\Delta T\dot{Y}_n,$$
$$\dot{Y}_{n+1}=\dot{Y}_n[1-\tfrac{1}{2}(\Omega\Delta T)^2]-\Omega\Delta T\dot{X}_n$$

to calculate forward for the velocity components. To obtain ΔT, the Taylor expansion

$$\Delta X=\Delta T\dot{X}_n+\tfrac{1}{2}\Omega\dot{Y}_n(\Delta T)^2$$

was solved. An alternative method which avoided the intervention of ΔT by using the angle, ϕ, of the trajec-

TABLE II. Depression of field and transition layer thickness, L.

	$1-\Omega_\infty$				L	
S	Computed	Eq. (37)	Error	Fractional error	Computed	Eq. (38)
0.01	0.01571	0.01583	0.00012	0.008	2.0	2.02
0.03	0.0485	0.0483	−0.0002	−0.004	2.1	2.05
0.05	0.0817	0.0819	0.0002	0.002	2.1	2.08
0.10	0.1708	0.1718	0.0010	0.005	2.2	2.19
0.15	0.2709	0.2728	0.0019	0.007	2.35	2.31
0.20	0.3838	0.3903	0.0065	0.017	2.5	2.47
0.25	0.5227	0.5367	0.0140	0.027	2.75	2.71
0.28	0.6264	0.6531	0.0267	0.043	3.0	2.91

tory with the x axis was used later for the case where lighter particles (electrons) were included in the plasma.

The problem was set up on the Univac.

B. Quantities Remembered and Univac Limitations

The quantities stored for final typing were Ω at all reference planes and Y and T for completed trajectories.

The fast storage of the Univac limited the number of active trajectories to 60 and this is the number present in a field $\Omega=20/60=0.333$. The value of S which will give this field is readily found from the relation

$$S=\frac{1-\Omega_\infty^2}{\pi}=\frac{1-1/9}{\pi}=0.2829, \quad (37)$$

which follows fairly directly from Eqs. (23) and (31).

Undue caution in setting up the problem led to not using all possible digit positions so that the results were not as accurate as had been hoped for. Answers are good to better than 5% as will be seen in the presentation of results.
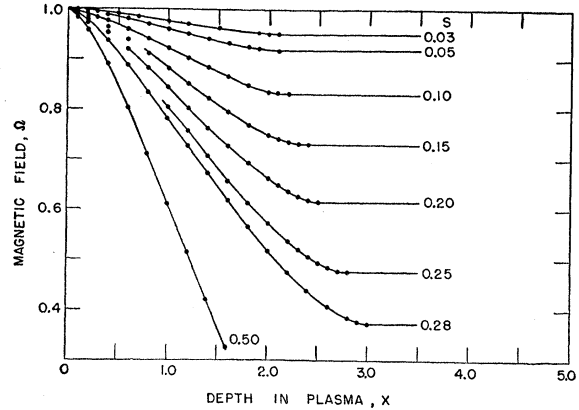
FIG. 5. Transition layer at the edge of a single-speed-particle plasma.

C. Weak Plasma

Table I shows the comparison between theory and calculation for a weak plasma. The quantities compared are (1) ultimate depression of the field, $\Delta\Omega_\infty$, where the plasma becomes uniform, which is after one Larmor diameter, (2) the time for a complete orbit, τ, taken for the first trajectory, i.e., $H=0$, and (3) the drift, Y_0, of the orbit in one cycle, also for the first orbit. It is here that agreement seems to be least satisfactory, but it must be noted that the total y excursion of the trajectory is two radii, that is, 2, so that with respect to this quantity the error is only 2.4%, about the same as the error in $\Delta\Omega_\infty$.

D. Depression of Field

Equation (37) furnished a check on the ultimate depression of the field as given by the Univac. Table II shows the results. The error relative to the depression of the field by the plasma is shown in the fifth column.

E. Thickness of Transition Layer

What was surprising was the rapidity and definiteness with which the final field value was reached. This is shown by the curves of Fig. 5 which give the course of the magnetic field with depth into the plasma. Even when the reduction of field is to 0.374 where the number of live trajectories at any position is not quite trebled, there is still a definite termination to the transition region.

Although it has not been possible to derive an expression for the transition layer thickness, L, from the theory, the results show a simple empirical relation which is exact within the accuracy of the computations:

$$L=\frac{4}{1+(1-\pi S)^{\frac{1}{2}}}. \quad (38)$$

This is the diameter of an orbit in a field which is the average between that in the vacuum and in the fully

developed plasma. The numerical comparison between the computed layer thickness and the Eq. (38) thickness appears in the last two columns of Table II.

F. Period in Uniform Plasma

In all cases where the Univac ran long enough before the automatic stop operated, so that the first reference trajectory which lay entirely in the uniform plasma was completed, it was possible to compare the computed half-period $\tau/2$ with π/Ω_∞. Since the computed field showed some variability in this range, a mean value was used. In the third and fourth column of Table III are the computed half-period of the trajectory and its diameter. The fifth column is the averaged field over the orbit found by averaging the field at perigee, center, and apogee. The last two columns contain, respectively, the corresponding half-period and the comparison with Column 3.

G. Paramagnetic Drift Current

Finally the results have been used to compute the paramagnetic drift current, J_2. This should result from summing X/τ for all trajectories. This was done for $S=0.25$ and the computation gave 0.2842. The Univac gave

$$\Omega_\infty = 0.4773,$$

whence by Eq. (36)

$$J_2 = 0.2862,$$

a check to within 0.5%. The formula Ω_∞ for $S=0.25$ is 0.4633 from Table II and this leads to $J_2=0.3109$, a difference of some 8%.

It may be important that the transition layer can be as thin as has been found possible here. If Eq. (38) can be extrapolated—an admittedly dangerous business— we find that the transition layer can be very thin relative to the orbital diameter in a strong plasma. Even within the range of the computation this ratio has fallen to about one-half. Undoubtedly this is a consequence of the fact that the trajectory curvature adapts immediately to the local field.

X. NUMERICAL SOLUTIONS OF PLANE CASE INCLUDING ELECTRONS

If we identify the particles we have been dealing with as positive ions, it is of interest to go on to examine the

TABLE III. Relation between period and field.

S	H_u[a]	Half-period $\tau/2$	Space intervals in diameter $20\Omega_\infty^{-1}$	Average field $\bar{\Omega}_\infty$	Half-period $\pi\bar{\Omega}_\infty^{-1}$	Relative defect in period
0.10	22	3.766	23	0.8289	3.790	−0.006
0.15	24	4.391	27	0.7108	4.420	−0.007
0.20	25	5.093	32	0.6142	5.115	−0.004
0.25	28	6.621	42	0.4732	6.639	−0.003

[a] H_u is the ordinal number of the first reference trajectory to lie entirely in a uniform field.
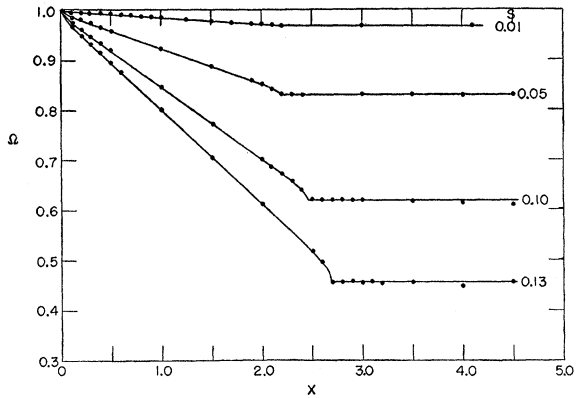
FIG. 6. Transition layer at the edge of a composite plasma.

effect of including electrons in the analysis. The simplest assumption regarding their energy is that it is the same as that of the ions. Their velocities will then be of the order of 100 times that of the ions and their Larmor radii will be less by that factor. Therefore the electrons can smoothly accommodate to any distribution demanded by the less accommodating ions. In particular the anisotropy in electron velocity distribution will be two orders of magnitude less than that of the ions so that no purpose would be served in analyzing electron trajectories in the same detail as the positive ions. It is appropriate to use the slow-space-variation formula

$$j_e = m_e v_e^2 n_e'/(2B) \quad \text{(emu)} \tag{39}$$

for the electron-current density j_e arising from an electron-density gradient n_e'. For electrical neutrality, which we now invoke,

$$n_e(x) = n_p(x) = \frac{B_0^2}{4\pi m_p v_0^2} \int_{H(X)}^X \frac{S(H)\Omega(H)dH}{\dot{X}}, \tag{40}$$

with $n_p(x)$ now given by the right member of Eq. (23).

For the weak plasma case, Eq. (39) integrates directly to give the depression of the field due to the electrons:

$$\Delta_e B = -2\pi m_e \langle v_e^2 \rangle_{\text{Av}} n_e(x)/B_0.$$

In this case, by Eq. (27),

$$n_e(x) = n_p(x) = \frac{B_0^2 S}{4\pi m_p v_p^2}\psi,$$

where $\psi = \cos^{-1}(1-X)$ is the angle traversed by the ion. Now, combining and noting the assumed equality of energy, we have for the effect of the electrons

$$\Delta_e B/B_0 = \Delta_e \Omega = -\tfrac{1}{2}S\psi,$$

whereas for the effect of ions, we have Eq. (26). The electrons do, therefore, modify the shape of the field transition, making it more linear with angle and less

linear with x. In the present case,

$$\Omega - 1 = \Delta\Omega = -S(\psi - \tfrac{1}{4}\sin 2\psi). \tag{41}$$

Here S is the buildup function of the ions alone.

For the strong plasma case, B in Eq. (39) is not constant so that

$$\Delta_e B = -2\pi m_e \langle v_e^2 \rangle_{\text{Av}} \int_0^x \frac{n_e'}{B(x_1)} dx_1.$$

Since n_e', found by differentiating Eq. (40), involves three terms, it is more convenient to integrate by parts to obtain

$$\Delta_e B = -2\pi m_e \langle v_e^2 \rangle_{\text{Av}} \left[\frac{n_e(x)}{B(x)} + \int_0^x \frac{n_e(x_1)B'(x_1)}{B(x_1)^2} dx_1 \right].$$

By substituting for $n_e(x)$ from Eq. (40) and noting the equality of kinetic energy, we get

$$\Delta_e \Omega = -\frac{1}{2\Omega(X)} \int_{H(X)}^X \frac{S(H)\Omega(H)dH}{|\dot{X}|}$$
$$+ \int_0^X \frac{\Omega'(X_1)dX_1}{\Omega(X_1)^2} \int_{H(X_1)}^X \frac{S\Omega dH}{\dot{X}_1}, \tag{42}$$

$\Delta_p \Omega$ is given by Eq. (22) as before, but now

$$\Omega(X) = 1 + \Delta_e \Omega(X) + \Delta_p \Omega(X). \tag{43}$$

Application of the Univac to this generalized problem involved nothing essentially new.

The results of the Univac calculations parallel those of the last section.

Since each ion is now accompanied by an electron, the plasma arising from a value of S here is to be compared to that from a value $2S$ in the ion-only case. Figure 6 is a plot of the course of the magnetic field with depth into the plasma. A notable feature is the sharp initial and final drops in field which are presaged by the weak-field equation, Eq. (41).

Tables IV and V exhibit the same kinds of result for the ions-and-electron case as did Tables II and III for

TABLE IV. Depression of field and transition layer thickness, L.

	$1 - \Omega_\infty$				L	
S	Computed	$(1 - 2\pi S)^{\frac{1}{2}}$	Error	Fractional error	Computed	Eq. (38)
0.01	0.03183	0.03183	0	0	2.03	2.032
0.05	0.1698	0.1718	0.0020	0.012	2.19	2.188
0.10	0.3806	0.3904	0.0098	0.025	2.45	2.485
0.13	0.5436	0.5725	0.029	0.059	2.70	2.801

TABLE V. Relation between period and field.

S	H_u	$\tau/2$	$\bar{\Omega}_\infty$	$\bar{\Omega}_\infty \tau/2$
0.01	20.3	3.2493	0.96848	3.147
0.05	21.9	3.8174	0.82954	3.167
0.10	24.5	5.1226	0.61252	3.138
0.13	27.0	7.21 ?	0.43983	3.17 ?

the ions-only case. Here in Table IV, by treating the magnetic field near the end of the transition layer as if $(\Omega - \Omega_\infty)^{\frac{2}{3}}$ varied linearly with X (on a purely empirical basis), an interpolation for a fractional final interval was found and used in the L (computed) column.

In Table V, the comparison to be made is between the values in the last column and τ.

XI. CONCLUSION

The specific result of the present analysis is that the transition between vacuum and uniform plasma is not limited in sharpness by the orbit diameter in the uniform region but is fixed more nearly by the vacuum field. A strong plasma in which $8\pi nKT$ approaches B_0^2 need not therefore have an essentially thicker transition than a weak plasma in the same vacuum field, thus freeing the hydromagnetic approach from a possible limitation.

Somewhat more generally, the paramagnetic contribution of the particle drift in the boundary has been separated out from the predominant diamagnetic effect which, by the present method of accounting, arises from certain parts of circular orbits.

More generally, still, it has been possible to use the trajectory approach in a self-consistent mathematical description of a plasma in a magnetic field and to derive, in this way, relations hitherto derived by neglecting the structure imparted to the plasma by the orbital motion. In particular, the more fundamental role of the tensor nature of the pressure in the cylindrical as distinguished from the Cartesian case becomes very clear.

It will be necessary to solve many simple problems involving trajectories in as many ways as possible to gain the insight needed to solve some of the less simple problems which now confront us.

ACKNOWLEDGMENT